

Efficient room-temperature source of polarized single photons

REFERENCE TO RELATED APPLICATIONS

The present application claims the benefit of U.S. Provisional Application No. 60/438,769, filed January 9, 2003, whose disclosure is hereby incorporated by reference in its entirety into the present disclosure.

STATEMENT OF GOVERNMENT INTEREST

The research leading to the present invention was supported in part by the U.S. Army Research Office under Award No. DAAD19-02-1-0285. The work was also supported by the U.S. Department of Energy Office of Inertial Confinement Fusion under Cooperative Agreement No. DE-FC03-92SF19460. The government has certain rights in the invention.

FIELD AND BACKGROUND OF THE INVENTION

The present invention is directed to quantum information technology, e.g., quantum cryptography. It relates to an efficient, room-temperature source of polarized single photons and more particularly to such a source using deterministically aligned single emitters in a planar aligned liquid crystal host.

Quantum information in the form of quantum communications and quantum computing is an exceedingly active field today. See, for instance, the following books: M. A. Nielsen and I. L. Chuang, *Quantum computation and quantum information*, Cambridge: Cambridge Univ. Press, 2001, D. Bouwmeester, A. Ekert, A. Zeilinger, Eds., *The physics of quantum information: quantum cryptography, quantum teleportation, quantum computation*, Springer: Berlin, 2000, and the following review paper: N. Gisin, G. Ribordy, W. Tittel, and H. Zbinden, *Rev. Mod. Phys.*, vol. 74, 145. 2002. Numerous theoretical concepts promise powerful quantum-mechanics-

based tools that, to date, wait for realization pending the arrival of reliable hardware. A single-photon source (SPS) that efficiently produces photons with antibunching characteristics is one such pivotal hardware element for quantum information technology. Using a SPS, secure quantum communication will prevent any potential eavesdropper from intercepting a message without the receiver's noticing. (E. Klarreich, *Nature*, vol. 418, 270-272, 2002)

In another implementation, a SPS becomes the key hardware element for quantum computers with linear optical elements and photodetectors (See the following paper: E. Knill, R. Laflamme, and G.J. Milburn, *Nature*, vol. 409, 46-52, 2001). Again, its practical realization is held back in part by difficulties in developing robust sources of antibunched photons on demand.

In spite of several solutions for SPSs presented in the literature, significant drawbacks remain. They are the reason for current quantum communication systems being baud-rate bottlenecked so that photon numbers from ordinary photon sources may be attenuated to the single-photon level (~ 0.1 photon per pulse on average). An efficient (with an order of magnitude higher photon number per pulse) and reliable light source that delivers a train of pulses containing one and one photon only is a very timely challenge. To meet this challenge, several issues need addressing, from achieving full control of the quantum properties of the source to easy handling and integrability of these properties in a practical quantum computer and/or communication setup. In addition, in quantum information systems it is desirable to deal with single photons synchronized to an external clock, namely, triggerable single photons. Polarization states of single photons are also important as they enable polarization-qubit encoding of information.

The critical issue in producing single photons by a method other than by trivial attenuation of a beam is the very low concentration of photons emitters dispersed in a host, such that within

a laser focal spot only one emitter becomes excited which can emit only one photon at a time. Most current SPSs, e.g., based on semiconductor heterostructures, operate only at liquid He temperature – a major impediment to widespread use. (See the following papers: J. Kim, O. Benson, H. Kan, Y.A. Yamamoto, *Nature*, vol. 397, 500-503, 1999; A. Imamoglu and Y. Yamamoto, *Phys. Rev. Lett.*, vol. 72, 210-213, 1994; E. Moreau, I. Robert, J. M. Gérard, I. Abram, L. Manin, V. Thiery-Mieg, *Appl. Phys. Lett.*, vol. 79, 2865-2867, 2001; P. Michler, A. Kiraz, C. Becher, W.V. Schoenfeld, P.M. Petroff, L. Zhang, E. Hu, A. Imamoglu, *Science*, vol. 290, 2282-2285, 2000; C. Santori, M. Pelton, G. Solomon, Y. Dale, and Y. Yamamoto, *Phys. Rev. Lett.*, vol. 86, 1502-1505, 2001; M. Pelton, C. Santori, J. Vučković, B. Zhang, G.S. Solomon, J. Plant, and Y. Yamamoto, *Phys. Rev. Lett.*, vol. 89, 233602, 2002; Z.L. Yuan, B.E. Kardynal, R.M. Stevenson, A.J. Shields, C.J. Lobo, K. Cooper, N.S. Beattie, D.A. Ritchie, M. Pepper, *Science*, vol. 295, 102-105, 2002).

Of the known room-temperature (RT) SPSs, only those based on single-dye-molecule fluorescence can be used in much higher speed systems than other RTSPSs. This SPS was developed in the following papers: W. P. Ambrose, P.M. Goodwin, J. Enderlein, D.J. Semin, J.C. Martin, R.A. Keller, *Chem. Phys. Lett.*, vol. 269, 365-370, 1997; L. Fleury, J.-M. Segura, G. Zumofen, B. Hecht, and U.P. Wild, *Phys. Rev. Lett.*, vol. 84, 1148-1151, 2000; B. Lounis and W.E. Moerner, *Nature*, vol. 407, 491-493, 2000; F. Treussart, A. Clouqueur, C. Grossman, and J.-F. Roch, *Opt. Lett.*, vol. 26, 1504-1506, 2001; F. Treussart, R. Alleaume, V. Le Floch, L.T. Xiao, J.M. Courty, J.F. Roch, *Phys. Rev. Lett.*, vol. 89, no. 9, 093601-4, 2002, and in the US Patent Application Publication No. 2002/0146052 A1, October 10, 2002 by W.E. Moerner and B. Lounis. Alternatives such as color centers in diamond and colloidal semiconductor CdSe-ZnS quantum dots possess unacceptably long fluorescence lifetimes. For instance, the diamond color

center has a 11.6-ns and 22.7 ns fluorescence life time in mono- and polycrystal, and CdSe-ZnS quantum dots one of ~ 22 ns. (See, for example, the following papers: C. Kurtsiefer, S. Mayer, P. Zarda and H. Weinfurter, " *Phys. Rev. Lett.*, vol. 85, 290-293, 2000; R. Brouri, A. Beveratos, J.-P. Poizat and P. Grangier, *Opt. Lett.*, vol. 25, 1294-1296, 2000; A. Beveratos, R. Brouri, T. Gacoin, J.-P. Poizat, and P. Grangier, *Phys. Rev. A*, vol. 64, 061802(R), 2001; A. Beveratos, S. Kuhn, R. Brouri, T. Gacoin, J.P. Poizat, P. Grangier, *Europ. Phys. Journ. D*, vol. 18, 191-196, 2002; A. Beveratos, R. Brouri, T. Gacoin, A. Villing, J.P. Poizat, P. Granger, *Phys. Rev. Lett.*, vol. 89, no. 18, 187901-4, 2002; P. Michler, A. Imamoglu, M.D. Mason, P.J. Carson, G.F. Strouse, and S.K. Buratto, *Nature*, vol. 406, 968-970, 2000; B. Lounis, H.A. Bechtel, D. Gerion, P. Alivisatos, W.E. Moerner, *Chem. Phys. Lett.*, vol. 329, 399-404, 2000; G. Messin, J.P. Hermier, E. Giacobino, P. Desbiolles, and M. Dahan, *Opt. Lett.*, vol. 26, 1891-1893, 2001).

The key advantage of dye molecules is that their excited-state life-time of only a few nanoseconds permits excitation repetition rates above ~ 100 MHz. In dye-based SPSs, one of the current challenges is dye bleaching. However, recently single terrylene molecules have been doped into p-terphenyl molecular crystals (10^{-11} moles of terrylene per mole of p-terphenyl) prepared by a sublimation procedure that produced tiny platelets. In this host, the dye is protected from exposure to diffusing quenchers (such as oxygen), and benefits from strong phonon emission into the host, preventing rapid thermal decomposition of the dye under intense illumination (B. Lounis and W.E. Moerner, *Nature*, vol. 407, 491-493, 2000; the US Patent Application 20020146052 A1, October 10, 2002 by W.E. Moerner and B. Lounis; L. Fleury, J.-M. Segura, G. Zumofen, B. Hecht, and U.P. Wild, *Phys. Rev. Lett.*, vol. 84, 1148-1151, 2000). For "thick" p-terphenyl crystals (~ 10 μm), this system becomes extremely photostable, allowing

hours of continuous illumination of individual molecules without photobleaching. It assures long-term spectral stability and reproducibility from one terrylene absorber to the next. Pumped by periodic, short-pulse laser radiation, single photons were generated at predetermined times at pump-pulse-repetition rates within the accuracy of the emission lifetime (~ 3.8 ns). Technical
5 implementation of this system is difficult as these monoclinic, sublimation-produced microcrystals are stress sensitive and fragile. In addition, terrylene's molecular dipole moment in the p-terphenyl host crystal takes on an orientation perpendicular to the platelet's surface (i.e., perpendicular to the incident light's E-field). This, in turn, leads to poor coupling with the polarized excitation light, prompting poor fluorescence emission even at high excitation
10 intensities (saturation intensity is about 1 MW/cm^2 at room temperature).

In spite of the elegance of the terrylene/p-terphenyl experiments, this technology must be considered unrealistic for practical application. Its weak point is also a background from "ordinary photons" from out-of-focus molecules or Raman scattering, because of the very high pumping intensities required. Emitted photons are not polarized deterministically (there is no
15 known, efficient method for aligning rapidly a multitude of micrometer-sized, monoclinic crystallites relative to one another). Note that noncrystalline, amorphous hosts, e.g., polymers, do not (1) offer the same spectral stability in single-molecule emission even in the case of terrylene, (2) provide long-time protection against bleaching. To date, no crystal hosts other than the fragile, sublimated p-terphenyl flakes have been proposed in single-dye-molecule room-
20 temperature experiments.

SUMMARY OF THE INVENTION

It is an object of the present invention to overcome the above deficiencies.

It is in particular an object of the invention to produce deterministically polarized single photons.

5 It is another object of the invention to do so with a high efficiency.

It is another object of the invention to do so at room temperature.

It is still another object of the invention to do so in such a way that provides long-term protection against bleaching.

10 It is yet another object of the invention to do so in a way which is suitable for practical applications.

To achieve the above and other objects, the present invention provides new approaches towards an implementation of an efficient, deterministically polarized SPS: (1) using aligned liquid-crystal hosts of either monomeric or oligomeric/polymeric form to preferentially align the single emitters for maximum excitation efficiency. Deterministic emitter alignment will also
15 provide deterministically polarized output photons; (2) using planar-aligned cholesteric liquid crystal hosts as 1-D photonic-band-gap microcavities tunable to the emitter fluorescence band to further increase SPS efficiency; (3) using liquid crystal technology to prevent emitter bleaching. Emitters comprise soluble dye molecules, inorganic nanocrystals or trivalent rare-earth chelates.

The present invention uses single emitters; that is, all emitters should be separated from
20 each other without any aggregate formation with two or more emitters together. Only one emitter should be excited within a focal volume (e.g., ~ 1 emitter/cubic micron concentration).

It is preferable that the emitter be selected from the group of compounds exhibiting sufficient solubility in the host at or near room temperature. In that context, throughout the

disclosure including the claims, it will be understood that "sufficient solubility" is solubility sufficient to provide single emitter concentration. Such sufficient solubility may be low in absolute terms, but it will be sufficient if it meets the above criterion.

BRIEF DESCRIPTION OF THE DRAWINGS

A preferred embodiment of the present invention will be set forth in detail with reference to the drawings, in which:

FIG. 1 is a diagram showing the manner in which a planar cholesteric for visualization purposes can be described as consisting of a layered structure and also showing transmission and reflection of a circular polarized light by a 1-D photonic band gap cholesteric liquid crystal layer near selective reflection conditions;

FIG. 2 is a perspective view of the topographical image (1120 nm x 1120 nm) for a particular liquid crystal platelet which was cut from a planar-aligned Wacker oligomer cholesteric liquid crystal (OCLC) coating on the substrate and flipped on its side;

FIG. 3 is a graph showing selective reflection of left-handed circularly polarized light from photonic band gap Wacker OCLCs;

FIG. 4 is a graph showing selective reflection of right-handed circularly polarized light from photonic band-gap E7 + CB15 monomeric mixture. *Planar alignment was made with the buffing method;*

FIG. 5 is a graph showing selective reflection of right-handed circularly polarized light from photonic band gap E7 + CB15 monomeric mixture. *Planar alignment was made with the photoalignment method;*

FIG. 6 is a schematic diagram of a device for testing the output of a sample photon source according to the preferred embodiment;

FIGs. 7A and 7B are fluorescence images of samples in which single terrylene molecules are embedded in a Wacker OCLC host and in which clusters of terrylene molecules spin coated onto a bare glass cover slip; respectively (10 μm x 10 μm scan);

FIG. 8 is a diagram of a three-level system for modeling the operation of the preferred embodiment;

FIGs. 9A and 9B are coincidence events histograms from host-free single terrylene molecules and an assembly of many uncorrelated molecules within an excitation volume, respectively;

FIGs. 10A and 10B are histograms of coincidence events of the single-terrylene-molecule-fluorescence on a bare glass substrate and of the radiation of scattered light from the excitation laser beam; respectively;

FIGs. 11A and 11B are histograms of coincidence events of the single-terrylene-molecule-fluorescence in a Wacker OCLC host and of an assembly of several uncorrelated molecules, respectively; and

FIG. 12 is a plot of fluorescence bleaching behavior of an assembly of terrylene molecules as a function of time and in two different liquid-crystal hosts: with oxygen depletion (upper curve), and without its depletion (lower curve).

15

DETAILED DESCRIPTION OF THE INVENTION

A preferred embodiment of the invention and experimental results therefrom will now be set forth in detail with reference to the drawings.

For visualization purposes, planar cholesterics (chiral nematics) can be described as consisting of a layered structure (although physically they do not have such a structure). For example, as shown in FIG. 1, a planar-aligned cholesteric 100 can be viewed as made up of a plurality of layers 102, of which expanded views showing the molecular orientations are shown as 104. The axes A of the molecular director (rightmost set of arrows) rotate monotonically to form a periodic helical structure with pitch P_0 . When a solid, planar-aligned cholesteric is flipped on its side and inspected by a high-resolution tool such as an atomic-force-microscope, the periodic pitch becomes observable through height variations along the helical axis. For instance, FIG. 2 shows such a topography for a Wacker cyclo-tetrasiloxane-oligomer cholesteric liquid-crystal (OCLC) platelet. It was cut from a planar-aligned OCLC coating on the substrate. Periodic stripes in the image correspond to one half of the pitch length.

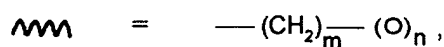
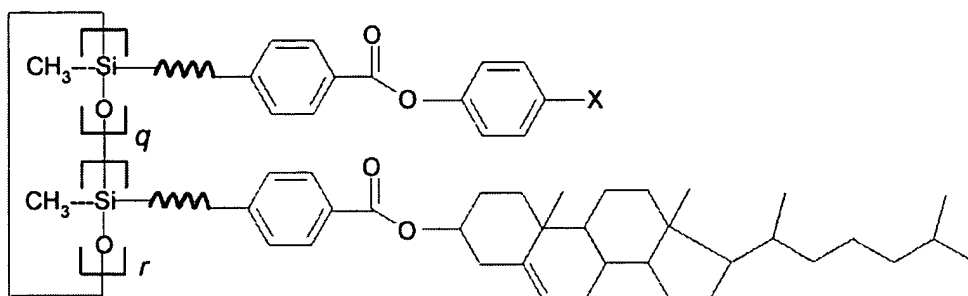
With few exceptions, liquid-crystal media are non-chiral and require additives to induce the chiral order. Dependent on the chirality-inducing additive, the final structure may show either a right- or a left-handed sense of rotation. For liquid-crystal thicknesses $\geq 10 \mu\text{m}$, the reflectance of normally incident, circularly polarized light with electric-field vector-rotation opposite to the rotation of molecules in the helical structure (Bragg condition), approaches 100% within a band centered at $\lambda_0 = n_{av}P_0$ where $n_{av} = (n_e + n_o)/2$ is the average of the ordinary and extraordinary refractive indices of the medium. This is the so-called selective reflection of cholesteric liquid crystals. In the example of FIG. 1, incident unpolarized light L_U with λ_0 is incident on the chiral nematic 100, and a right-hand circularly polarized component is reflected as right-hand circularly

polarized light L_{RH} , while a left-hand circularly polarized component is transmitted as left-hand circularly polarized light L_{LH} . The bandwidth is $\Delta\lambda = \lambda_0 \Delta n / n_{av}$, where $\Delta n = n_e - n_o$.

Such a periodic structure can also be viewed as a 1-dimensional photonic crystal, with a band gap within which propagation of light is forbidden. For emitters located within such a structure, the rate of spontaneous emission is suppressed within the spectral stop band and enhanced near the band edge. Several groups have reported lasing in photonic band gap material hosts, including cholesteric liquid crystals (I.P. Il'chishin, E.A. Tikhonov, V.G. Tishchenko and M.T. Shpak, *JETP Lett.*, vol. 32, 24-27, 1980; V.P. Kopp, B. Fan, H.K.M. Vithana and A.Z. Genack, *Opt. Lett.*, vol. 23, 1707-1709, 1998; H. Finkelman, S.T. Kim, A. Munoz, P. Palffy-Muhoray, B. Taheri, *Adv. Mater.*, vol. 13, no. 14, 1069-1072, 2001).

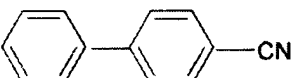
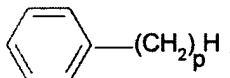
Generation of strongly circularly polarized photoluminescence from planar-aligned cholesteric liquid crystals was also reported in the following papers: S.H. Chen, D. Katsis, A.W. Schmid, J.C. Mastrangelo, T. Tsutsui, T.N. Blanton, *Nature*, vol. 397, 506-508, 1999; D. Katsis, A.W. Schmid, S.H. Chen, *Liq. Cryst.*, vol. 26, 181-185, 1999; A.Yu. Bobrovsky, N.I. Boiko, V.P. Shibaev, J.H. Wendorff, *Adv. Mater.*, vol. 15, no. 3, 282-287, 2003.

In the experiments to be described herein, monomeric liquid crystal mixtures with a chiral additive, and Wacker siloxane OCLC were doped with terrylene or other dye at extremely low concentration such that the final sample contained only a few molecules per μm^2 irradiation area. Wacker siloxane OCLC has the following formula:

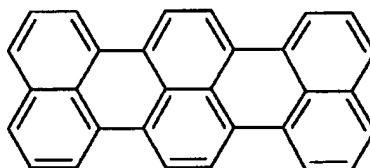


where $m = 3, 4, 5, 6, 8, 10$ and $n = 0, 1$

$q + r = 3, 4, 5, 6$ or 7 and $q/(q + r) = 0$ to 1

$X = \text{Cl}, \text{OMe}, \text{O}(\text{CH}_2)_3\text{H},$  or , where $p = 2, 4$ or 5

while terrylene has the following formula:



To prepare the 1-D photonic band-gap structures three different planar alignment procedures for liquid crystals were used: (i) substrate shearing, (ii) buffing, (iii) and photoalignment. Two alternate methods were also found satisfactory for planar alignment: either the film was flow aligned by letting the OCLC solution run down a vertically inclined glass slip, or a special glass-cylinder was rolled unidirectionally across a spin-coated OCLC heated to the liquid state ($\sim 100^\circ \text{C}$) and slowly cooled afterwards.

For sheared samples, no additional substrate coatings were needed. For buffing, substrates were spin coated with either of two polymers: Nylon-6 or Polyimide. For buffing, we used a standard, velvet-surface buffing machine. Single-molecule fluorescence microscopy imposes a

requirement on the sample thickness: ~ 180 and $300\ \mu\text{m}$ -working distance of high N.A. objectives permits use only of samples with thickness not exceeding this value. For this reason, $\sim 170\text{-}\mu\text{m}$ -thickness glass microscopic cover slip substrates (Corning) were used that both are fragile and need special care in handling. To prevent damage to the fragile substrates during the buffing procedure, cover slips were “blocked to” 1-mm-thick microscope slides with water-soluble acetate, using 40-min heating at 80°C for better results. After buffing, the cover slips were unblocked in standing, deionized water over night. This was followed by a rinse in flowing, deionized water to rid the samples of acetate traces.

For photoalignment, substrates were spin-coated with Staralign. Photoalignment of coated polymer was achieved using six, UV discharge lamps RPR 3000 (Southern New England Ultraviolet Co.) with maximum wavelength $\sim 302\ \text{nm}$ (40 nm bandwidth) and a UV linear dichroic polarizer (Oriel), 1.74” x 1.74” large, placed in a hermetic box. The photoalignment procedure at $\sim 5\ \text{mW}/\text{cm}^2$ power density at 302 nm lasted 10 minutes.

We used two types of liquid crystals to prepare layers ranged in thickness from 50 nm to 30 micrometers. In addition to Wacker oligomer cholesteric-liquid-crystal powders described earlier, mixtures of low molecular weight, E7 nematic liquid crystal blend with a chiral additive CB15 were used. Both E7 and CB15 are fluids at room temperature. Both materials were supplied by EM Industries.

For the Wacker oligomer liquid crystal powders, the samples were prepared by mixing different concentration of two powders with individually known selective-reflection wavelengths provided by the vendor. In order to obtain a desired selective-reflection wavelength mixture, mixing rules were found empirically from a set of multiple, different mixtures. To change the pitch of each mixture, powders were dissolved in methylene chloride, mixed for 2 hours under

agitation and at elevated temperature, purified through a 0.45- μm particle filter, and dried from solvent under vacuum. For planar alignment an uncoated, cleaned cover slip with a Wacker powder was placed on a hot plate and melted at $\sim 100^\circ\text{C}$. A second cover slip was used to shear the melted oligomer at temperature (and to also form the second window of the liquid-crystal cell). Slowly cooling the cell to room temperature froze in the planar alignment. For some Wacker powders, we used spin coating with Polyimide and buffing of substrates. Cells with known and uniform thickness (10 – 15 μm) were created by using 4 drops of a UV-cured epoxy mixed with calibrated, glass-bead spacers at the substrates corners. After that, cells containing Wacker powder were heated into the isotropic phase and slowly cooled.

For low-molecular-weight liquid crystals, the coated substrate surfaces were either buffed or photoaligned. Cell thickness was again set by UV-epoxy mixed with glass-bead spacers. To find the weight concentration of the components C in a mixture of chiral additive and nematic liquid crystal with desired selective reflection wavelength λ_o we used a well-known relationship $C = n_{av}/(\lambda_o \times HTP)$, where HTP is the helical twisting power of the chiral additive in a nematic liquid crystal. For CB15 in E7, $HTP \approx 7.3 \mu\text{m}^{-1}$. An E7 + CB15 liquid crystal mixture with selected concentration was fed through a 0.45- μm particle filter and a stainless-steel syringe into the assembled cell parallel to the polymer-alignment direction inscribed in the cell walls.

We prepared several tens of planar-aligned cholesteric liquid crystal samples with band gaps in different spectral regions (λ_o varied from 430 nm to 2200 nm). We used a Perkin Elmer Lambda 900 spectrophotometer to measure the wavelength response of each prepared sample, thereby determining the specific selective reflection (photonic band gap) for each sample. A zero-order quarter wave plates and a thin-film linear polarizer were used in both spectrophotometer channels to create circularly polarized incident light of desired handedness.

Samples were tested in unpolarized, as well as in left-handed, and right-handed circularly polarized incident light. FIG. 3 shows transmittance of Wacker oligomer cholesteric-liquid-crystal samples versus wavelength in left-handed circularly polarized light. In these experiments, we used both pure Wacker OCLCs with selective reflection bands centered around 450 nm, 535 nm and 760 nm, and mixtures of two OCLCs possessing selective reflection closest to the desired wavelength.

Similar results were achieved with the E7 + CB15 mixture, both with buffed Polyimide/Nylon-6 (FIG. 4) and with photoalignment (FIG. 5), in right-handed circularly polarized light (handedness strictly determined by the CB15 structure).

To minimize false fluorescence contributions by contaminants during single-molecule-fluorescence microscopy, rigorous cleaning of glass substrates is mandatory. Liquid-crystal cells were fabricated in a class 10,000 liquid-crystal clean-room facility. Ultrasonic cleaning for 60 minutes freed the 1" x 1" substrates from any dirt particles. Substrates were then rinsed in flowing, deionised water, dried in a stream of compressed nitrogen and washed in toluene from organic components. To remove the toluene substrates were washed again with pure ethanol and dried. After that, they were etched in piranha solution ($\text{H}_2\text{SO}_4 + \text{H}_2\text{O}_2$ in equal volume concentration) for about 20 minutes, rinsed in flowing, deionized water and dried in a stream of oil-free nitrogen.

Proper terrylene concentration for single-molecule fluorescence microscopy was established by iterative trial and error. In sequential dilution steps of terrylene in chlorobenzene solvent, solutions were spun onto glass slips, and for each concentration, confocal fluorescence microscopy determined the final emitter concentration per irradiation volume. Once single molecules were predominantly observed, the dilution endpoint was reached. This final terrylene

solution was mixed with Wacker OCLC starting material (8% weight concentration of oligomer), E7 + CB15 or 5CB + CB15 mixtures.

Terrylene's fluorescence maximum lies near 579 nm with a bandwidth of ~ 30 nm. FIG. 3 (dotted curves) shows matching the cholesteric liquid crystal's λ_o to the dye-fluorescence band, but in our current experiments we used Wacker OCLC with $\lambda_o = 2.2 \mu\text{m}$, i.e., outside the terrylene-dye-fluorescence band. The liquid crystal was doped with terrylene at an extremely low concentration, such that the final sample contained only a few molecules per μm^2 irradiation area.

Single molecule fluorescence microscopy and photon antibunching correlation measurements are carried out using a setup 600 shown in FIG. 6. Antibunching is the evidence of a single photon nature of the source. The terrylene-doped liquid crystal sample 602 is placed in the focal plane of a 0.8 N.A. microscope objective of a confocal microscope (Witec alpha-SNOM platform) 604. The sample is attached to a piezoelectric, XYZ translation stage 606. Light emitted by the sample is collected by a confocal setup using a 1.25 N.A., oil-immersion objective 608 and an interference filter 610 together with an aperture in form of the 50- μm -core optical fiber 612.

The cw, spatially filtered through a fiber, linearly polarized (contrast $10^5:1$), 532-nm diode-pumped Nd:YAG laser output 614, excites single molecules. In focus, the intensities used are of the order of several kW/cm^2 .

The collection fiber 612 is part of a non-polarization-sensitive 50:50 fiber splitter 616 that forms the two arms of a Hanbury Brown and Twiss correlation setup. Residual, transmitted excitation light is removed by the interference filter 610 (formed of two, additively placed,

dielectric interference filters), yielding a combined rejection of better than 6 orders of magnitude at 532 nm.

Photons in the two Hanbury Brown and Twiss arms 618, 620 are detected by identical, cooled avalanche photodiodes 622, 624 in single-photon-counting Geiger mode (SPCM-AQR-14-FC, Perkin Elmer Optoelectronics, Vaudreuil, Canada). The time interval between two consecutively detected photons in separate arms is measured by a 68-ns-full-scale time-to-digital converter (Model 7186, Phillips Scientific) 626 using a conventional start-stop protocol. Within this converter's linear range, the time uncertainty in each channel corresponds to 25 ps.

It was proved experimentally that a very good approximation of the autocorrelation function $g^{(2)}(\tau)$ comes directly from the coincidence counts (event distribution) $n(\tau)$, for relatively low detection efficiency and therefore low counting rate. This justifies the assumption that $n(\tau)$ is proportional to the autocorrelation function $g^{(2)}(\tau)$. For single photons, $g^{(2)}(0) = 0$, indicating the absence of pairs, i.e., antibunching.

FIGs 7A and 7B show terrylene-dye-molecule-fluorescence images obtained by confocal fluorescence microscopy. FIG. 7A shows single terrylene molecule embedded in a Wacker OCLC host. FIG 7B shows clusters of terrylene molecules spin coated from chlorobenzene solution onto a bare glass cover slip. For both images, the scan direction is from left to right and line by line from top to bottom. The scan dimensions are 10 μm x 10 μm . Most single molecules in these samples exhibited fluorescence blinking in time, with a period ranging from several milliseconds up to several seconds. That "blinking" behavior by single molecules manifests itself as bright and dark horizontal stripes in the image. These features are absent in emission images from clusters. Blinking is a common phenomenon and convincing evidence of the single-photon nature of the source. Several mechanisms are suggested for the explanation of blinking behavior,

for instance, “shelving” (triplet blinking) to the long-living state, and fluctuations in the photo-physical parameters of the molecule and its local environment.

By modeling the molecule as a three-level system (singlet ground state S_0 , excited state level S_1 , and triplet state T_1) as depicted in FIG. 8, triplet blinking can be explained by a population buildup at the T_1 level that is often a dark state in fluorescent dyes. A single-pixel dwell time of ~ 8 ms does not allow resolution of the lifetime of this triplet state ($\sim 10^{-4}$ s for terrylene in a p-terphenyl). The second mechanism is more plausible for the explanation of long-time intensity fluctuations although the details are not clearly understood.

FIG. 9A and 9B show a coincidence-count histogram $n(\tau)$ from host-free single terrylene molecules on a bare glass substrate (FIG. 9A) and an assembly of many uncorrelated molecules within the excitation volume (FIG. 9B).

The scan speed is ~ 3 s per line (512 pixels). The left histogram exhibits a dip at $\tau = 0$. The measured signal-to-background ratio of our experiments ranges from 2 to 8, so the probability that a photon from the background triggers a coincidence with a photon from the molecule is very low.

Because $n(\tau)$ is proportional to the autocorrelation function $g^{(2)}(\tau)$, $n(0) \sim 0$ means that $g^{(2)}(0) \sim 0$ in the experiments. Two fluorescence photons are not observed within an arbitrarily short time interval. This fluorescence antibunching is due to the finite radiative lifetime of the molecular dipole and is therefore clear proof that we observed the emission from one and only one molecule. The histogram of FIG. 9B from multiple, uncorrelated molecules shows no such dip at $\tau = 0$, i.e., no antibunching.

To eliminate any potential for leaked excitation light causing the dip at $\tau = 0$, the sample was replaced with a bare glass slide and one blocking interference filter was removed. The

coincidence histogram for this condition is depicted in FIG. 10B. No antibunching is observed. The results are shown in FIG. 10A and 10B, which bear the same relation to each other as do FIG. 9A and 9B.

FIG. 11A and 11B show the results of doping terrylene into liquid crystals. The histogram of coincidence events $n(\tau)$ (FIG. 11A) exhibits a dip at $\tau = 0$, indicating photon antibunching in the fluorescence of the single molecules in the Wacker OCLC host; no antibunching is observed in the fluorescence from an assembly of several uncorrelated molecules in the same host, different sample (FIG. 11B). FIG. 11A is noteworthy in that it demonstrates that several single molecules can sequentially contribute to an antibunching histogram without loss of $\tau = 0$ contrast, as in practice the long integration time and competing molecule-bleaching events make obtaining an entire, good-contrast histogram from only one molecule too much a matter of luck. When the initial single molecule was bleached, the sample was advanced to another single molecule while the photon-correlation count continued. This finding is crucial for future device implementation.

Practical device implementation also depends on photochemical stability of both emitters and hosts. Terrylene fluorescence stability in monomeric liquid crystal hosts was increased by saturating, prior to cell assembly, the liquid crystals with helium in a sealed glove-box for one hour. Oxygen that is mostly responsible for dye bleaching is displaced by helium during this procedure. FIG. 12 shows fluorescence-bleaching results of terrylene molecules at two-orders-of-magnitude higher concentration than in single-molecule experiments in different liquid crystal hosts: either immobilized in an oligomer cholesteric liquid crystal or dissolved in monomeric cyanobiphenyl 5CB saturated with helium (both at identical excitation intensity and identical terrylene volume concentration). Over the course of more than one hour, no dye bleaching was observed in the oxygen - depleted liquid crystal host (upper curve). Dye bleaching was avoided

also in the following paper: L.A. Deschenes and D.A. Vanden Bout, *Science*, vol. 292, 255-258, 2001 for ~ 1 hour of irradiation by placing the sample under nitrogen during a single-molecule excitation.

Dye bleaching is not a critical impairment for an efficient SPS, but it is an important factor for device simplicity and cost. When one molecule is bleached the system can be rapidly realigned to utilize another isolated dye molecule, allowing practically continuous source action (see FIGs. 9A, 10A, and 11A).

A robust room-temperature single-photon source based on fluorescence from a single-dye-molecule (fluorescence antibunching) was demonstrated for the first time for liquid crystal hosts. Planar-aligned, 1-D photonic-band-gap structures in dye-doped cholesteric oligomers were prepared. Avoiding bleaching of the terrylene dye molecules for excitation times > 1 hour was achieved by innovative preparation procedures.

Estimating the efficiency of the SPS using conservative value of parameters, a comparison was made of the number of exciting 532-nm photons/s N_{inc} incident on the absorption cross-section area σ of a terrylene molecule with a measured photon counting rate from a single molecule $N_{out} = 3kc/s$. For the laser power incident on the sample $\sim 17.5 \mu W$, a beam radius $\sim 0.25 \mu m$, and using measured value of $\sigma \sim 5 \times 10^{-17} cm^2$ for terrylene molecules provides $N_{inc} = 1.2 \times 10^6$ photons/s-mol.

A probability p_a can be evaluated for a single photon to be emitted into an optical fiber core of the Hanbury Brown -- Twiss setup of FIG. 6, from the following expression: $2N_{out} = 0.95N_{inc} p_a DQ$. Here $D = 0.2$ is the measured coupling efficiency of the fiber optics used in this setup, $Q = 0.64$ is the photon detection efficiency of the avalanche photodiode (APD) at 579 nm, 0.95 is the coupling efficiency from the fiber to the APD-FC-connector. Those data provide p_a

≈4%. This rather surprisingly large value is strongly dependent on the measured absorption cross-section for which we used a conservative estimate.

These results can be improved to take advantage of the capabilities offered by the liquid crystal host to increase the excitation and collection efficiency. It can be estimated how the probability p_a might be improved. For instance, the count rate may be increased at least by 2.6 – 4.3 times by the alignment of the liquid crystal/dye molecules relative to the incident polarization. The efficiency improves a factor between two and three with the microcavity compared to the dye molecules without the cavity. It is safe to say that an SPS efficiency increase of up to one order of magnitude can be expected using planar alignment of a cholesteric host whose photonic band gap matches the dye fluorescence band.

The probability of two-photon emission P_2 is approximately $P_2 = C_N(0)P_1^2/2$ if P_2 is much smaller than unity. P_1 is the probability for single photon emission; $C_N(0)$ is the zero time normalized coincidence rate that can be taken directly as the correlation function $g^{(2)}(0)$. For Poissonian light $C_N(0) = 1$. For single terrylene molecule fluorescence in a Wacker oligomer liquid crystal host, $C_N(0) = 0.25 - 0.33$. It means that the rate of two-photon pulses is three - four times lower than for Poissonian light. It should be noted that a probability p_a introduced earlier, $p_a = \alpha P_1$. Here α is a collection efficiency including losses in filters.

Other possible modifications include increasing the efficiency, life, and polarization purity of the single photon source by improved selection of dye, liquid crystal, and the photonic-band-gap structure matching with the dye fluorescence band. A pulsed laser source can be used to create a real quantum cryptography system with a cholesteric liquid crystal single-photon source on demand.

While a preferred embodiment of the present invention has been set forth above, those skilled in the art who have reviewed the present disclosure will readily appreciate that other embodiments can be realized within the scope of the present invention. Various examples of such other embodiments are mentioned above. Moreover, disclosures of specific liquid crystal hosts are illustrative rather than limiting; any suitable monomeric or oligomeric/polymeric liquid crystal host can be used, and those skilled in the art who have reviewed the present disclosure will readily be able to select an appropriate host. Similarly, disclosures of specific emitters are illustrative rather than limiting. For example, current colloidal semiconductor nanocrystal technology, for instance, using PbSe quantum dots of specific size provides single emitters with a fluorescence in a spectral region between 1000 and 2200 nm, in particular at the communication wavelengths of 1300 and 1500 nm. These quantum dots can be easily dissolved in liquid crystals. Also, numerical values and disclosures of specific hardware are illustrative rather than limiting. For instance, a pulsed laser source can be used to trigger SPS on demand. Therefore, the present invention should be construed as limited only by the appended claims.

15